# Characteristics of a New Gas-Induced Reactor

**Yung-Chien Hsu and Chyuan-Jih Huang**
Dept. of Chemical Engineering & Technology, National Taiwan Institute of Technology, Taipei, 10672, Taiwan, R.O.C.

*A newly developed gas-induced reactor for gas-liquid heterogeneous reactions presented here has no baffle on the inner wall of the tank body. Inside the reactor tank, two in-series 45° pitched blade downward turbines enclosed by a draft tube were employed. As the turbines rotate at high speeds, a central gas vortex is formed downwardly along the central shaft from the free surface of the liquid toward the upper turbine. The gas is then induced by the upper turbine and mixes with the input gas. After that, the mixed gas is broken into bubbles by the lower turbine and dispersed through the liquid vortex. With the formation of gas and liquid vortexes, the reactive gas was able to circulate in the liquid phase to achieve high gas utilization. The experimental studies were on the heterogeneous ozonation reaction of a reactive dye (C.I. Reactive Blue 19). Major experimental parameters, such as impeller speed, input concentration of ozone, input flow rate of ozone and liquid volume, were changed to investigate the characteristics of the gas-induced reactor. This gas-induced reactor achieved high gas utilization ratio, short reaction time, and high recovery of the unreactive gas.*

## Introduction

Many reactors such as bubble columns, packed columns, plate columns, ejector mixers, Venturi scrubbers, and agitated tanks have been employed in the industry. They all have their own merits and drawbacks when used for gas-liquid reaction systems (Charpentier, 1981; Shah et al., 1982; Rice and Browning, 1981; Bollyky, 1981). The agitated tank is one of the most important reactors widely used for gas-liquid heterogeneous reactions in the chemical industry. For proceeding a gas-liquid reaction, an agitated tank should have the characteristics of good mixing effect, mass transfer, heat transfer, low power consumption, and long gas/liquid contact time, and so on. Especially for the gas-liquid reaction systems, the design of reactor configuration is one of the key factors.

In general, a flat blade Rushton turbine, gas sparger, and four baffles are usually used to achieve the ability of gas dispersion and fluid mixing for gas-liquid reaction in a conventional agitated tank (Oldshue, 1983; Charpentier, 1981; Joshi, 1982). This type of the agitated tank provides good performance. However, the interaction between the Rushton turbine and baffles requires high power consumption. Furthermore, the recovery of the unreactive gas injected through the process liquid from the bottom of the tank is complicated in the agitated tank. This problem is frequently solved by linking a series of tanks or using a compressor to circulate the unreacted gas back to the process liquid. Both of these two methods are complex processes and will increase the accessory equipment and operation costs. Also, the sparger tends to become blocked in case of containing solid phase. Although the above mentioned agitated tank is one of the most commonly used reactors for gas-liquid reaction systems, improvements in configuration for specific purposes such as simplifying the system to obtain better gas utilization, lower power consumption, and longer gas/liquid contact time are required.

The major purpose of this study is to develop a new reactor for recycling of unreacted gas that has escaped from the liquid surface during the gas-liquid reaction. In the reactor, a draft tube was employed owing to its good abilities of flow control and gas/liquid contact (Oldshue, 1983). Two in-series 45° pitched blade downward turbines enclosed by a draft tube were employed due to their lower power consumption at high impeller speed (Chapman, 1983; Oldshue, 1983), better gas dispersion, mixing effect and retention time (Warmoeskerken, 1984; Mann, 1986; Chapman, 1983; Bujalski and Nienow, 1990). The space between two turbines was set at one times of turbine's diameter to achieve stable gas induction and lower power consumption (Hsu and Chang, 1995; Oldshue, 1983).

Correspondence concerning this article should be addressed to Y.-C. Hsu.

To compare with the condition without gas induction, the effect of the gas induction can enhance the mass transfer between gas and liquid phase (Calderbank, 1959; Matsumura, 1979). While the turbines swirled at proper impeller speeds, a central gas vortex and free liquid vortex were easily formed in the reactor. The gas above the liquid surface was sucked into the gas vortex and was broken into bubbles by the two turbines. This action is called gas induction in this study. Owing to its gas induction ability, accessory equipment such as a compressor are not necessary for this type of gas-induced reactor. In view of a complete reactor unit including reactor and accessory equipment, a decrease in the total costs can be expected for the use of this studied reactor to treat the gas of slow reactions.

## Theoretical Background

### *Mass-transfer model*

The heterogeneous ozonation reaction can be divided into two major categories of mass-transfer-controlled and reaction-controlled reactions (Rice and Browning, 1981; Gould and Ulirsch, 1992). Both of these two categories of reaction can proceed in the gas-induced reactor. This study focused on the first one to simplify the evaluation of the reactor. For a mass-transfer-controlled ozonation reaction similar to the case used in this experiment, owing to the low solubility of ozone, the resistance of gas film diffusion is negligible as compared with that of liquid film diffusion, and the rate of mass transfer of ozone from gas phase into liquid phase is limited by liquid film diffusion (Kuo et al., 1977; Sotelo et al., 1989; Gould and Ulirsch, 1992; Munter et al., 1993). By referring to Saunders et al. (1983), Gould and Ulirsch (1992) applied a model based on Levenspiel's equation for the heterogeneous ozonation of dyes and nitrated phenols with an associated instantaneous chemical reaction (Levenspiel, 1972). We can assume that gas-phase resistance is negligible for the ozonation of reactive dye presented in Eq. 1; then, the rate of reaction can be defined by Eq. 2 (Saunders et al., 1983).

$$\text{dye} + b\text{O}_3 \rightarrow \text{product} \tag{1}$$

$$-r'_d = Sk_{L,\text{O}_3}\left(\frac{D_{L,d}C_d}{D_{L,\text{O}_3}} + \frac{P_{\text{O}_3}}{bH_{\text{O}_3}}\right) \tag{2}$$

Saunders et al. (1983) also showed that the second term ($P_{\text{O}_3}/bH_{\text{O}_3}$) is negligible as compared with the first term. ($P_{O_3}$ is the partial pressure of ozone in gas input, kPa, $H_{\text{O}_3}$ is the Henry's constant of ozone, kPa/mole frac., and $-r'_d$ is the reaction rate of dye, mol/s). Therefore, Eq. 3 can be obtained by dividing Eq. 2 by the liquid volume $V$

$$-\frac{dC_d}{dt} = \frac{k_{L,\text{O}_3}aD_{L,d}}{D_{L,\text{O}_3}}C_d \tag{3}$$

Equation 3 is consistent with the first-order ozonation kinetics of dyes (Hoigne and Bader, 1983a,b). Assuming that the diffusivity of ozone and dye in water and the quantity of $k_{L,\text{O}_3}a$ remain constant during the reaction, Eq. 4 is obtained by integrating Eq. 3 ($k_{L,\text{O}_3}$ is the mass-transfer coefficient of ozone in liquid film, m/s)

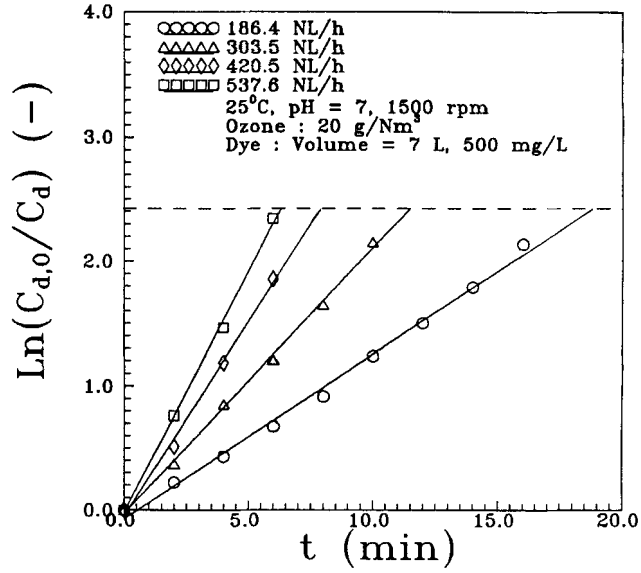


**Figure 1. Experimental results by the relationship of Eq. 4.**

$$\ln\frac{C_{d,o}}{C_d} = \frac{k_{L,\text{O}_3}aD_{L,d}}{D_{L,\text{O}_3}}t \tag{4}$$

The value of $\ln(C_{d,o}/C_d)$ at any time in a reaction is plotted against the reaction time as shown in Figure 1. ($C_d$ is concentration of dye in liquid (mg/L) and $C_{d,o}$ is the initial dye concentration (mg/L).) In Figure 1, the linear relationship between $\ln(C_{d,o}/C_d)$ and the reaction time $t$ (min) show that the ozonation of experimental dye is a first-order mass-transfer control reaction until the concentration of residual dye reaches 10% of the initial concentration. The slope of the straight line in Figure 1 represents $k_{L,\text{O}_3}aD_{L,d}/D_{L,\text{O}_3}$. Quoting the Wilke-Chang equation (Wilke and Chang, 1955) and Eq. 5 (Matrozov, 1976) to calculate the molecular diffusivity of dye ($\text{m}^2/\text{s}$) $D_{L,d}$ and the molecular diffusivity of ozone in liquid film ($\text{m}^2/\text{s}$) $D_{L,\text{O}_3}$, the values are $1.54\times10^{-9}$ $\text{m}^2/\text{s}$ and $1.42\times10^{-9}$ $\text{m}^2/\text{s}$, respectively. The overall mass-transfer coefficient $k_{L,\text{O}_3}a$ (1/s) can then be obtained to assess the reaction rate of the heterogeneous ozonation of experimental dye ($T$ is the temperature of liquid ($k$) and $\mu$ is the viscosity of liquid (kg·m/s))

$$\frac{D_{L,\text{O}_3}\mu}{T} = 4.27\times10^{-15} \tag{5}$$

Furthermore, Sotelo et al. (1989) and Benitez et al. (1993) applied the two-film theory to the ozonation of azo and sulfur dyes. They showed that if the reaction kinetics is first-order with respect to dye but pseudo $m$-th order with respect to ozone, the change of dye concentration during the reaction could follow the relationship of Eq. 6 as follows

$$1-(C_d/C_{d,o})^{0.5} = k't \tag{6}$$

where

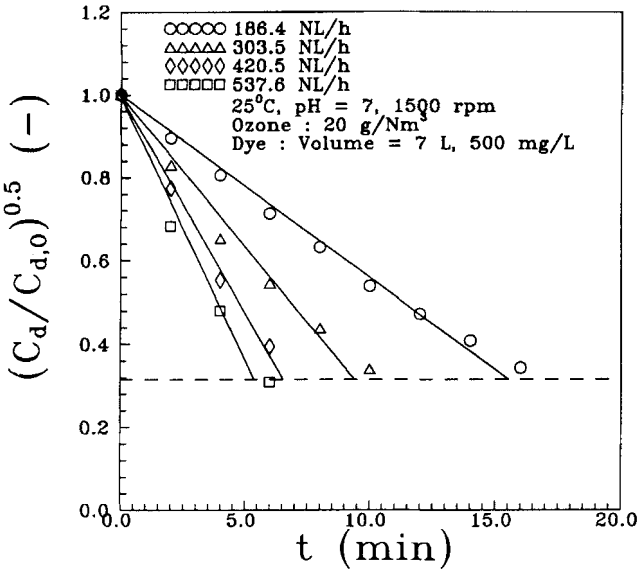


**Figure 2. Experimental results by the relationship of Eq. 6.**

$$k' = \frac{a}{2b}\sqrt{\frac{2kD_{O_3}(C^*_{O_3})^{m+1}}{C_{d,o}(m+1)}} \qquad (7)$$

In Eq. 7, $C^*_{O_3}$ is the ozone equilibrium concentration (mol/L), and $k$ is the kinetic rate constant ($L^{0.5}/mol^{0.5}\cdot s$) ($m$ is the order of reaction with respect to the ozone.) For such reactions, the following can be observed and concluded:

(1) Ozone reacts with the dye very quickly.

(2) During the initial period of reaction, ozone almost only reacts with the dye due to the high concentration of the dye, so that the interfering reaction of ozone with intermediate products can be neglected.

Referring to Figure 2, the results of this experiment conform to Eq. 6 well until the concentration of residual dye reaches 10% of the initial one. At the final stage of reaction, the dye concentration is relatively low so the reactions between ozone and subproducts become relatively more significant, and the value of $D_{L,d}/D_{L,O_3}$ may no longer be a constant. To simplify the performance evaluation of the reactor, this experimental study adapts those experimental data before the ratio of $(C_d/C_{d,o})$ reaches 0.1.

### *Definition of ozone utilization ratio*

In this study, the ozone utilization ratio is defined by Eq. 8

$$U_{O_3} = \frac{W_{O_3,in} - W_{O_3,out}}{W_{O_3,in}} \times 100\% \qquad (8)$$

where $W_{O_3,in}$ and $W_{O_3,out}$ are the total input and output amounts of ozone measured in gas phase (g). A higher $U_{O_3}$ presents a better utilization of ozone. This experimental study performed the decoloration reaction by ozone and hydroxyl radical OH· formed from the self-decomposition of ozone (Hoigne and Bader, 1983a,b; Staehelin and Hoigne, 1985). The ozone utilization ratio calculated from the gas phase would include all the ozone consumption by the two ozonation pathways (molecular and radical). However, the loss of ozone by decay is negligible.

## Experimental Studies

Ozonation of the reactive dye C.I. Reactive Blue 19 (Constitution no.: C.I. 61200) was used to evaluate the performance of the gas-induced reactor. The RB19 dye (product of Sumitomo Chemical Co. Ltd.) has a wavelength of maximum absorption at 589 nm. Dye solution with a concentration of 500 mg/L was loaded into the reactor. The pH value of the dye solution was controlled at 7 by 0.2 M sodium hydroxide solution during the reactions. The temperature of the reactor was maintained at $25 \pm 0.1$°C.

Figure 3a shows the proto-configuration of the gas-induced reactor, and indicates the type of each element and its relative position. The cylindrical tank body with a flat bottom was made of acrylic resin. Its inner diameter was 170 mm with a height of 700 mm, and a thickness of 5 mm. The inner

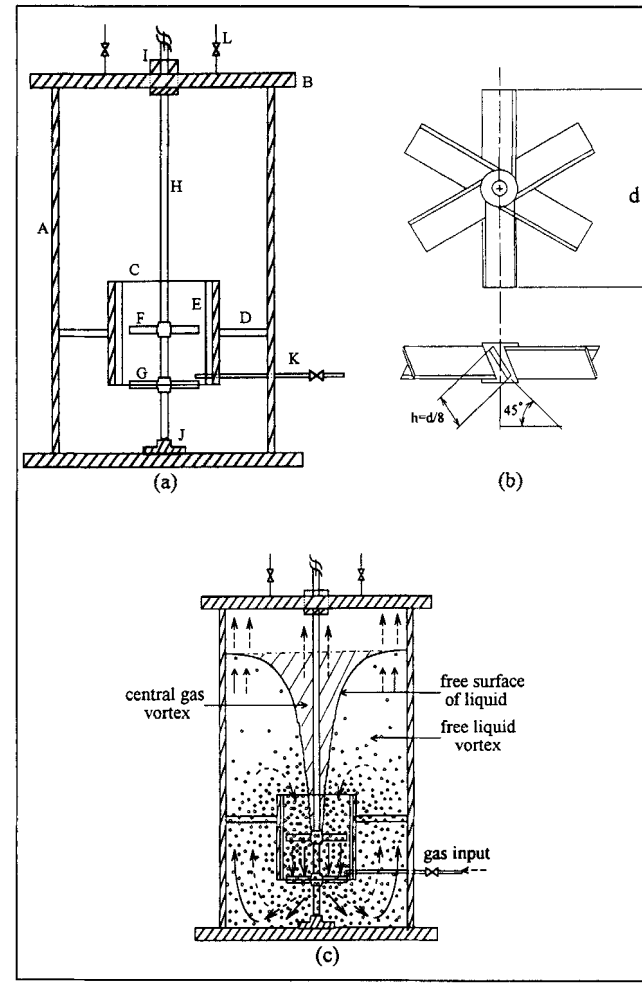


**Figure 3. Descriptions of the gas-induced reactor.**

(a) Configuration of the gas-induced reactor—(A) tank body, (B) top cover, (C) draft tube, (D) cylindrical bracket, (E) inner baffles, (F) upper turbine, (G) lower turbine, (H) shaft, (I) mechanical seal, (J) support, (K) input for ozone, (L) gas output; (b) Configuration of the 45° pitched blade downward turbine; (c) Flow paths of gas and liquid in the gas-induced reactor at gassing condition (---> : gas,— > : liquid).

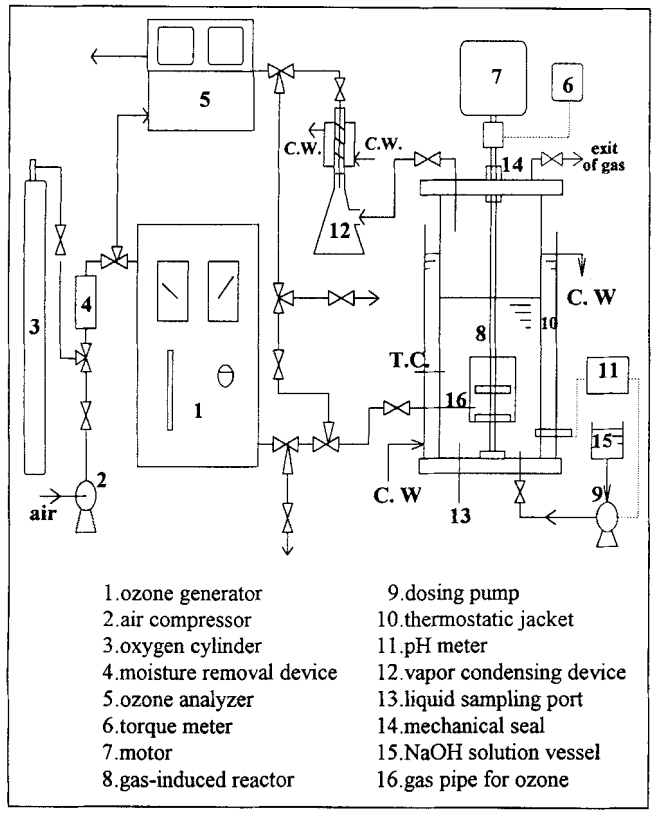


1.ozone generator
2.air compressor
3.oxygen cylinder
4.moisture removal device
5.ozone analyzer
6.torque meter
7.motor
8.gas-induced reactor
9.dosing pump
10.thermostatic jacket
11.pH meter
12.vapor condensing device
13.liquid sampling port
14.mechanical seal
15.NaOH solution vessel
16.gas pipe for ozone

**Figure 4. Experimental apparatus.**

diameter of the cylindrical draft tube was 80 mm with a length of 120 mm and thickness of 5 mm. The bottom end of the draft tube was located 75 mm above the flat bottom of the reactor. Four baffles were symmetrically and perpendicularly fixed on the inner wall of the draft tube. Their width was 1/20th of the draft tube's inner diameter. Both of the two turbines had a diameter of 60 mm (refer to Figure 3b). The distance between the two turbines was 60 mm, and the plane of the lower turbine was level with the lower end of the draft tube. The shaft was driven by a motor and its end was inserted into a support which was mounted on the center of the flat bottom to prevent vibration of the shaft. The outlet of the gas pipe was located between the two turbines and near the lower turbine to introduce the fresh gas directly.

The experimental apparatus is shown in Figure 4. Fresh air or high purity oxygen was used as the feed gas for the ozone generator (Trailigaz Model LABO 76). The dosage of ozone applied to the system could be controlled by adjusting the effluent gas-flow rate or input voltage of the ozone generator. Ozone concentration in the gas phase was measured with the ozone UV photometry analyzer using a wavelength of 254 nm. The detection frequency of the analyzer could be set at a mode of 60 times per min or 3 times per min. Dye solution was sampled and determined periodically by the means of the UV/Visible photometer using a wavelength of 589 nm, and then the concentration of dye solution can be obtained in accordance with Lambert-Beer's law. The torque value of the shaft was measured with a torque meter to calculate the power consumed during the reaction. Moreover, a tracer study was done for evaluating the mixing time of the reactor (Krishna Murthy and Elliott, 1992).

During the experiment, most of the liquid samples were too concentrated to be analyzed by UV/Visible photometer. The solution was therefore diluted to enable analysis. Major errors in results probably occurred during the dilution process. Errors also occurred due to the stability of the ozone generator. However, the reproductivity of measured data is still good. The repeated experiment had a maximum $\pm 5\%$ error of the measured dye concentration, and $\pm 0.6\%$ error of ozone utilization ratio measured by means of the maximum, minimum, and average input ozone concentration.

## Results and Discussion

### *Flow pattern observation*

The phenomena of gas induction and bubble circulation exist at gassing and nongassing conditions when the gas-induced reactor is operated at high impeller speeds. In the case of nongassing condition (not shown), no central gas vortex was observed at lower turbine speeds ( $< 800$ rpm). As the speed of turbine was raised above 1,100 rpm, a regular central gas vortex was formed at the center of the liquid surface above the draft tube. There was no surging and vibration of the reactor. The regular vortex of gas was pulled inward to the draft tube by the two turbines and was then disturbed by inner baffles to become an irregular shape. This irregular gas vortex was then easily broken into bubbles by the upper turbine. The bubbles were then driven downwardly by the downward force in the draft tube and broken again and distributed angularly out of the draft tube by the lower turbine. Bubbles were then visually observed to flow up spirally through the annular area between the draft tube and tank inner wall. A large amount of bubbles was pulled toward the central shaft by the free liquid vortex formed by the fast rotation of dual turbines. They were then drawn inwardly over the upper end of the draft tube and forced back through the draft tube for further utilization. This phenomenon produced a forced circulation for gas bubbles. Only a small portion of gas bubbles, which were next to the wall, moved spirally upward and reached the free surface of the liquid. When these bubbles escaped the liquid phase, some quantity of gas was sucked back into the liquid phase by the central gas vortex. This circulation phenomena of the gas therefore also promoted a better gas utilization ratio. Figure 3c indicates the flow patterns of gas and liquid at the gassing condition. The fresh reactive gas was introduced to the area between the two fast rotating turbines. In the experimental observation, most of the reactive gas bubbles were circulating around the draft tube, so the reactive gas could be utilized efficiently by these two major functions.

Furthermore, in the tracer studies, the time required to reach 95% homogeneity are below 15 s at all of the experimental conditions of stable gas induction. Therefore, the good mixing effect can still be obtained at high impeller speed since the fast flow of bubbles and liquid increase the gas/liquid contact time. In addition, this reactor can be applied in other batch reactions, for example, hydrogenation of oil and fat. Pure hydrogen can be introduced to the upper gas phase and the supply of pure hydrogen may be controlled by a pressure regulating control valve. The flow patterns of gas and liquid will be similar to the nongassing condition observed in this experimental study.

### *Effects of impeller speed*

Impeller speed is the major factor affecting the behavior of the gas-induced reactor. In this bench-scale experimental equipment, as the impeller speed is raised up to 800 rpm, an unstable central gas vortex forms at the center of the liquid surface. The gas vortex can be intermittently broken into bubbles by two turbines. Consequently, experimental observation has shown the critical impeller speed to be 800 rpm. At impeller speeds of over 1,100 rpm, a stable gas vortex forms. A large amount of gas is induced into liquid phase and a large number of bubbles are circulated around the draft tube, so the conditions of the gas induction now appear. In the experimental results, at impeller speeds between 800–1,100 rpm, an increase in the impeller speed can increase the number of bubbles and decrease the bubble size. The heterogeneous ozonation rate of dye, the ozone utilization ratio, and the mass-transfer coefficient of ozone all increase. However, if the impeller speed is above 1,100 rpm, impeller speed has no obvious effect on the above mentioned three values because mass transfer reaches its limit. As shown in Figure 5, the mass-transfer coefficients of ozone are plotted against impeller speeds at three different liquid volumes. Sotelo et al. (1989) had reported similar results in the agitated tank. In their work, the effect of impeller speed on the solubility of ozone increased only slightly at high speeds. Therefore, for this experimental equipment, if the impeller speed is increased above 1,100 rpm, power will be wasted.

### *Effects of input quantity of ozone*

The input quantity of ozone can increase either with an increase in concentration at a constant flow rate or an increase in flow rate at a constant concentration. In the experimental results, the dye concentration decreases quickly as the input ozone concentration increases at a constant flow rate. The driving force of mass transfer is enhanced due to a high ozone concentration in the gas bubbles provided from a high input quantity of ozone. Similar results were also reported by

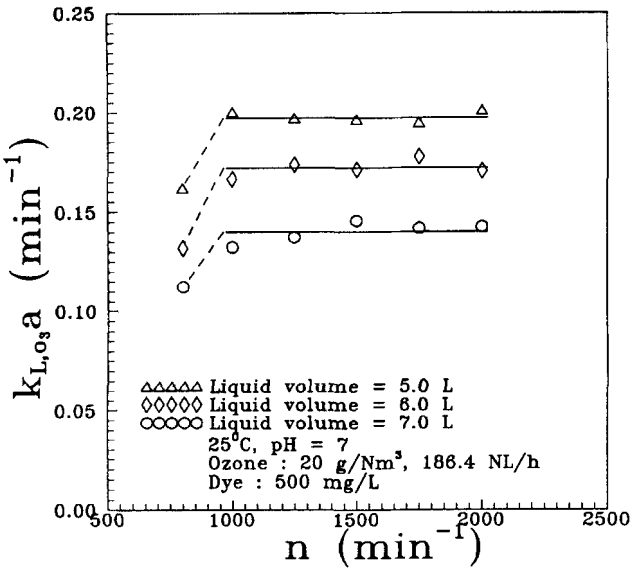


**Figure 5. Effect of impeller speed on mass-transfer coefficient for three different liquid volumes.**

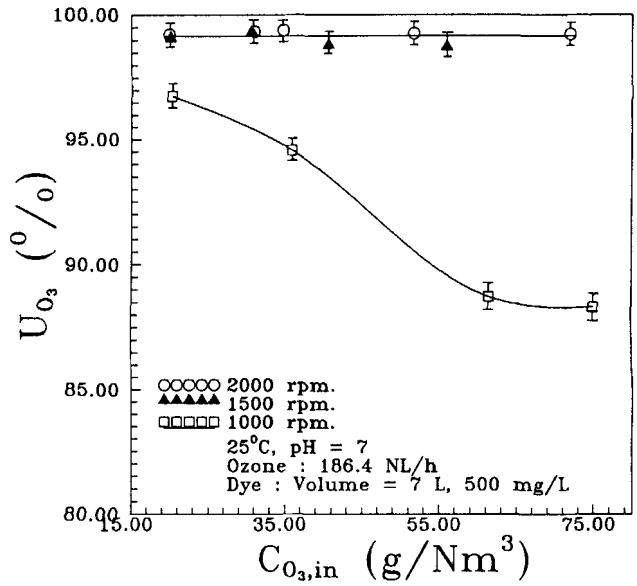


**Figure 6. Effect of input ozone concentration on ozone utilization ratio for three different impeller speeds.**

Sotelo et al. (1989) and Benitez et al. (1993). Figure 6 shows that most of the ozone utilization ratios are above the excellent level of 98% (except for the case of unstable gas vortex at 1,000 rpm before the dye concentration has decreased by 90%). Furthermore, the decoloration rate of RB19 dye can be increased with an increase in the input ozone flow rate at constant concentration. However, this does affect the efficiency of the reaction. As noted in Table 1, at a constant or different dosing rate, the ozone utilization ratios decrease with the increase in the input ozone flow rate. For example, the gas utilization decreases from 99% to 85% with respect to the input flow rate increases from 186 to 540 NL/h. This effect is more significant at lower impeller speeds. This is due to the trailing vortex found at the tip of the impeller blade as the reactor is operated at low impeller speed and high gas-flow rate (Smith, 1985). More fresh input gas buoys up through the draft tube and then leaves the liquid surface. At the same time, the retention of ozone in the dye solution decreases. Therefore, in the experimental gas-induced reactor, a smaller ozone flow rate with high concentration provides a higher ozone utilization ratio.

**Table 1. Effects of Input Quantity of Ozone on Ozone Utilization Ratio and Power Consumption for Agitation at Constant Impeller Speed**

| Input Ozone Flow Rate NL/h | Input Ozone Conc. g/N·m$^3$ | Ozone Dosing Rate g$O_3$/h | Ozone Utiliz. Ratio % | *P/V* kW/m$^3$ |
|---|---|---|---|---|
| 186.4 | 29.65 | 5.53 | 98.54 | 0.456 |
| 186.4 | 19.90 | 3.71 | 98.86 | |
| 303.6 | 18.30 | 5.56 | 96.63 | 0.401 |
| 303.6 | 20.04 | 6.08 | 96.92 | |
| 420.5 | 13.46 | 5.66 | 94.46 | 0.383 |
| 420.5 | 20.02 | 8.42 | 90.27 | |
| 537.6 | 10.20 | 5.48 | 91.14 | 0.365 |
| 537.6 | 19.89 | 10.69 | 84.22 | |

Note: impeller speed = 1,250 rpm; liquid volume = 7 L.

**Table 2. Effects of Liquid Volumes on Reaction Time and Ozone Utilization Ratio at Constant Ozone Dosing Rate**

| Liquid Vol. L | Liquid Level cm | Reaction Time s/L | Ozone Utiliz. Ratio % |
|---|---|---|---|
| 4.4 | 19.6 | 136 | 98.98 |
| 5.0 | 22.5 | 140 | 97.86 |
| 6.0 | 27.1 | 127 | 98.47 |
| 7.0 | 31.6 | 140 | 98.86 |

Note: impeller speed = 1,250 rpm; dosing rate of ozone = 3.73 $gO_3/h$; flow rate = 186.4 NL/h.

### *Effects of liquid volume*

Generally speaking, the reaction time of unit volume is usually shorter and utilization ratio is better at a low liquid volume in comparison to a high liquid volume. This is because the low liquid volume provides better turbulence. However, the experimental results indicate the effects of liquid volume are not particularly significant. Table 2 indicates the experimental results at different liquid volumes using same impeller speeds ($n$, r/min), dosing rate of ozone, and gas-flow rate. The required unit volume reaction time and ozone utilization ratio for decreasing 90% dye concentration is approximately the same. We infer the reasons of these results as follows. The circulation pathway of the bubbles and gas/liquid contact will increase with the increase in liquid volume. However, the ability for gas induction will be reduced by the increase in the submergence depth of two turbines. So, these two opposite influences lead to the result that the change of liquid volume seems to have no significant effect on the ozone utilization ratio. The gas-induced reactor may have the potential for flexibility of operational level in industrial application.

### *Power consumption for agitation*

The total power consumption in this experimental system consists of two parts—first, the production of ozone-containing gas by the ozone generator; second, agitation driven by the motor. The power consumption of the ozone generator accounts for more than 80% of the total power consumption. Therefore, an increased ozone utilization ratio has the benefit of saving operation cost in ozone generation.

Regarding power consumed for agitation, power consumption per unit volume of dye solution obtained at different liquid volumes is plotted against impeller speeds in Figure 7. As indicated, the power consumption for agitation increases with the increase in the impeller speed at different liquid volumes. However, different liquid volumes present slightly different power consumption at the same impeller speeds. Because no baffles are installed on the inner wall of the gas-induced reactor, the vortexes of gas and liquid remain stable. The inertia force of free liquid vortex increases with the increase in the liquid volume, so that the resistance to agitation decreases at high liquid volume. Consequently, the power consumption for agitation does not greatly increase with the increase in the liquid volume if the vortex of gas and liquid remain stable.

In Figure 8, the power consumption for agitation against input ozone flow rate is plotted at different impeller speeds. The figure indicates that the power consumption for agitation decreases slightly with the increase in flow rate at higher impeller speeds over the critical one. In the experimental observation, the gas induction ability of turbines was good at high impeller speeds, but the trailing vortexes are formed at the tip of the blades with an increase in ozone flow rate. This effect can be seen in Table 1. Many bubbles accumulate around two turbines especially at high input gas-flow rate. The power consumption for agitation thus decreases slightly with the increase in input gas-flow rate.

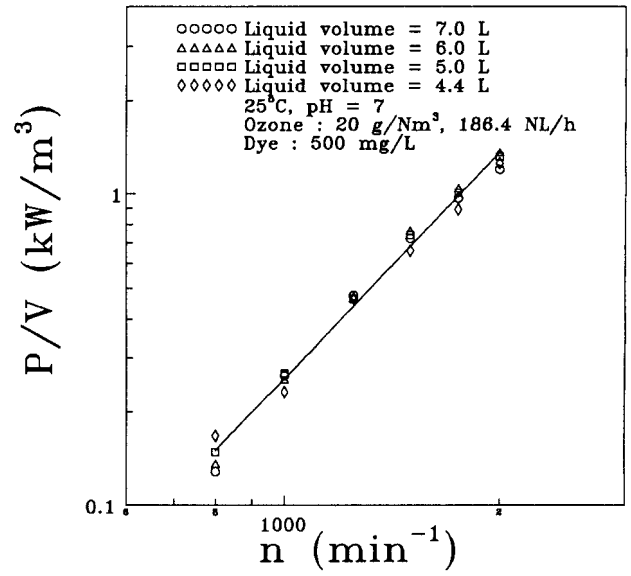


**Figure 7. Effect of impeller speed on power consumption for four different liquid volumes.**

To compare the gas-induced reactor with the conventional Rushton agitated tank, both at the condition of gassing and nongassing, power consumption of the gas-induced reactor is significantly lower than that of the Rushton agitated tank at the same impeller speeds. However, under the same ozone

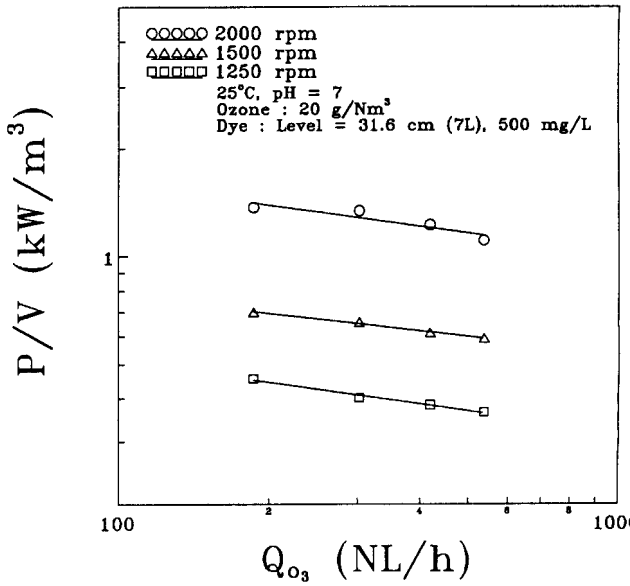


**Figure 8. Effect of input ozone flow rate on power consumption for three different impeller speeds.**

utilization ratio of 98%, the power consumption of the gas-induced reactor operated at high impeller speed (about 1,100 rpm) approximately equals that of the Rushton agitated tank operated at 600 rpm. Therefore, the gas-induced reactor requires high impeller speed to obtain the ability of gas induction, but the reactor will not require more power.

## Conclusion

In this article, we have presented a newly developed gas-induced reactor for gas-liquid reactions. The heterogeneous ozonation reaction of a RB19 dye was investigated to test the characteristics of the reactor. This reactor has the ability of gas induction to enhance the gas utilization. The operational impeller speed must be greater than the critical value of 800 rpm, and the suitable speed is approximately 1,100 rpm in this bench-scale experimental equipment. The input gas concentration has no significant effect on the gas utilization ratio at the condition of stable gas induction. The gas utilization ratio and power consumption decrease slightly with the increase in the input gas-flow rate at constant impeller speed over the critical one. Furthermore, the gas-induced reactor obtains excellent gas utilization at different liquid volumes. It appears to have the flexibility of operational liquid level and the ability to recover the unreactive gas in application. To compare with a conventional agitated tank, the studied reactor will not require as much power to obtain the ability of gas induction. Scale-up work is proceeding for further application.


## Acknowledgment

The authors thank the National Science Council of the Republic of China for its financial support under grant NSC84-2211-E-011-002.


## Notation

$a$ = specific gas-liquid interfacial area, $m^2/m^3$
$b$ = stoichiometric ratio
$P/V$ = power consumption per liquid volume for agitation, $kW/m^3$
$Q_{O_3}$ = flow rate of ozone, NL/h
$S$ = gas-liquid interfacial area, $m^2$

## Literature Cited


Benitez, F. J., J. Beltran-Heredia, T. Gonzalez, and A. Pascual, "Ozone Treatment of Methylene Blue in Aqueous Solutions," *Chem. Eng. Commun.*, **119**, 151 (1993).

Bollyky, L. J., "The Mass Transfer of Ozone into Water: Energy Requirements-State of the Art," *Ozone Sci. Eng.*, **3**, 181 (1981).

Bujalski, W., and A. W. Nienow, "The Use of Upward Pumping 45° Pitched Blade Turbine Impeller in Three-Phase Tanks," *Chem. Eng. Sci.*, **45**, 415 (1990).

Calderbank, P. H., "Physical Rate Processes in Industrial Fermentation: II. Mixing Transfer Coefficient in Gas-Liquid Contacting with and without Mechanical Agitation," *Instn. Chem. Engr.*, **37**, 173 (1959).

Chapman, C. M., A. W. Nienow, M. Cooke, and J. C. Middleton, "Particle-Gas-Liquid Mixing in Stirred Vessels: II. Gas-Liquid Mixing," *Chem. Eng. Res. Des.*, **61**, 82 (March 1983).

Charpentier, J. C., "Mass-Transfer Rates in Gas-Liquid Absorbers and Reactors," in *Advances in Chemical Engineering*, Vol. 11, Academic Press, New York, p. 2 (1981).

Gould, J. P., and G. V. Ulirsch, "Kinetics of the Heterogeneous Ozonation of Nitrated Phenols," *Wat. Sci. Technol.*, **26**(1-2), 169 (1992).

Hoigne, J., and H. Bader, "Rate Constants of Reactions of Ozone with Organic and Inorganic Compounds in Water: I. Non-Dissociating Organic Compounds," *Water Res.*, **17**, 173 (1983a).

Hoigne, J., and H. Bader, "Rate Constant of Reactions of Ozone with Organic and Inorganic Compounds in Water: II. Dissociating Organic Compounds," *Water Res.*, **17**, 185 (1983b).

Hsu, Y. C., and H. C. Chang, "Onset of Gas Self-Induction and Power Consumption after Gas Induction in Agitated Tank," *J. Chem. Tech. Biotechnol.*, **64**, 137 (1995).

Joshi, J. B., A. B. Pandit, and M. M. Sharma, "Mechanically Agitated Gas-Liquid Reactors," *Chem. Eng. Sci.*, **37**(6), 813 (1982).

Krishna Murthy, G. G., and J. F. Elliott, "Definition and Determination of Mixing Time in Gas Agitated Liquid Baths," *ISIJ Int.*, **32**(2), 190 (1992).

Kuo, C. H., K. Y. Li, C. P. Wen, and J. L. Weeks, "Absorption and Decomposition of Ozone in Aqueous Solutions," *AIChE Symp. Ser.*, **73**(166), p. 230 (1977).

Levenspiel, O., *Chemical Reaction Engineering*, 2nd ed., Wiley, New York (1972).

Mann, R., "Gas-Liquid Stirred Vessel Mixer: Toward a Unified Theory Based on Networks-of-Zone," *Chem. Eng. Res. Des.*, **64**, 23 (1986).

Matrozov, V. I., S. A. Kashtanov, A. M. Stepanov, and B. A. Tregubov, "Experimental Determination of the Molecular Diffusion Coefficient of Ozone in Water," *Zhur. Prikl. Khimii. (Soviet J. Appl. chem.)*, **49**(5), 1070 (1976).

Matsumura, M., H. Masunaga, and J. Kobayashi, "Gas Absorption in an Aerated Stirred Tank at High Power Input," *J. Ferment. Technol.*, **57**, 107 (1979).

Munter, R., S. Preis, S. Kamenev, and E. Siirde, "Methodology of Ozone Introduction into Water and Wastewater Treatment," *Ozone Sci. Eng.*, **15**, 149 (1993).

Oldshue, J. Y., *Fluid Mixing Technology*, McGraw-Hill, New York (1983).

Rice, R. G., and M. E. Browning, *Ozone Treatment of Industrial Wastewater*, Noyes Data Corp., NJ (1981).

Saunders, F. M., J. P. Gould, and C. R. Southerland, "The Effect of Solute Competition on Ozonolysis of Industrial Dyes," *Water Res.*, **17**(10), 1407 (1983).

Shah, Y. T., B. G. Kelkar, S. P. Godbole, and W. D. Deckwer, "Design Parameter Estimations for Bubble Column Reactors," *AIChE J.*, **28**, 353 (1982).

Smith, J. M., *Dispersion of Gases in Liquid: The Hydrodynamics of Gas Dispersion in Low Viscosity Liquids, Mixing of Liquid by Mechanical Agitation*, Gordon and Breach, New York, p. 139 (1985).

Sotelo, J. L., F. J. Beltran, F. J. Benitez, and J. Beltran-Heredia, "Henry's Law Constant for the Ozone-Water System," *Water Res.*, **23**(10), 1239 (1989).

Staehelin, J., and J. Hoigne, "Decomposition of Ozone in Water in the Presence of Organic Solutes Acting as Promoters and Inhibitors of Radical Chain Reactions," *Environ. Sci. Technol.*, **19**(12), 1206 (1985).

Warmoeskerken, M. M. C. G., and J. M. Smith, "Gas-Liquid Dispersion with Pitched Blade Turbine," *Chem. Eng. Commun.*, **25**, 11 (1984).

Wilke, C. R., and P. C. Chang, "Correlation of Diffusion Coefficients in Dilute Aqueous Solutions," *AIChE J.*, **1**, 264 (1955).



*Manuscript received Aug. 29, 1995, and revision received Apr. 8, 1996.*